Journal of Applied Fluid Mechanics, Vol. 8, No. 3, pp. 453-463, 2015.
Available online at www.jafmonline.net, ISSN 1735-3572, EISSN 1735-3645.
DOI: 10.18869/acadpub.jafm.67.222.22864

Heat and Mass Transfer by Unsteady Natural Convection over a Moving Vertical Plate Embedded in a Saturated Porous Medium with Chemical Reaction, Soret and Dufour Effects

S. M. M. EL-Kabeir, M. Modather and A. M. Rashad†

Department of Mathematics, Salman bin Abdulaziz University, College of Science and Humanity Studies, Al-Kharj, Saudi Arabia and Department of Mathematics, Aswan University, Faculty of Science, 81528, Egypt.

†*Corresponding Author Email: am_rashad@yahoo.com*

(Received March 29, 2014; accepted June 06, 2014)

ABSTRACT

The thermal-diffusion and diffusion-thermo effects on heat and mass transfer by transient free convection flow of over an impulsively started isothermal vertical plate embedded in a saturated porous medium were numerically investigated, considering a homogeneous chemical reaction of first order. The transient, nonlinear and coupled governing equations are solved using an implicit finite-difference scheme. The effects of various parameters on the transient velocity, temperature, and concentration profiles as well as heat and mass transfer rates are analyzed. Numerical results for the unsteady-state velocity, temperature and concentration profiles as well as the axial distributions and the time histories of the skin-friction coefficient, Nusselt number and the Sherwood number are presented graphically and discussed.

Keywords: Natural convection; Unsteady flow; Porous medium; Soret and Dufour effects; Chemical reaction.

1. INTRODUCTION

Combined heat and mass transfer problems on natural convection flow in a saturated porous medium have received considerable attention because of numerous applications in geophysics and energy related engineering problems. Such applications include natural circulation in geothermal reservoir, aquifers and porous insulations, packed bed reactors, sensible heat storage beds, and beds of fossil fuels such as oil shale and coal which have been fragmented for in situ energy extraction. The derivation of the empirical equations which govern the convective flow and heat transfer in porous media has been discussed by (Nield and Bejan 2006; Vafai 2000; Pop and Ingham 2001; Ingham and Pop 1998, 2002). Also, the growing need for chemical reactions in chemical and hydrometallurgical industries requires the study of heat and mass transfer with chemical reaction in porous medium which are of importance in many processes. There are many transport processes that are governed by the combined action of buoyancy forces due to both thermal and mass diffusion in the presence of the chemical reaction effect. These processes are observed in nuclear reactor safety and combustion systems, solar collectors, as well as metallurgical and chemical engineering. Their other applications include solidification of binary alloys and crystal growth dispersion of dissolved materials or particulate water in flows, drying and dehydration operations in chemical and food processing plants, and combustion of atomized liquid fuels. Diffusion and chemical reaction in an isothermal laminar flow along a soluble flat plate were studied by (Fairbanks and Wike 1950). Das *et al.* (1994) considered the effects of a first order chemical reaction on the flow past an impulsively started infinite vertical plate with constant heat flux and mass transfer. Muthucumarswamy and Ganesan (2001) have studied the first-order chemical reaction on flow past an impulsively started vertical plate with uniform heat and mass flux. The effects of permeability and chemical reaction on heat and mass transfer over an infinite moving plate in a saturated porous medium were reported by Modather *et al.* (2009). Rashad and EL-Kabeir (2010) have studied the coupled heat and mass transfer by transient mixed convection past a vertical stretching sheet embedded in a fluid-saturated porous medium in the presence of a chemical reaction effect. Rashad *et al.* (2011) have

also analyzed the MHD free convective heat and mass transfer of a chemically-reacting fluid from radiate stretching surface embedded in a saturated porous medium. Rashad *et al.* (2011) have also discussed the effect of chemical reaction on heat and mass transfer by mixed convection flow about a solid sphere in a saturated porous media. Chamkha *et al.* (2011) have investigated the effect of chemical reaction on heat and mass transfer by non-Darcy free convection from a vertical cylinder embedded in porous media. Muthucumaraswamy *et al.* (2013) have studied the effects of rotation and chemical reaction on the hydromagnetic free-convection flow of a fluid past a uniformly accelerated infinite isothermal vertical plate with variable mass diffusion. Chamkha *et al.* (2012) have analyzed the heat and mass transfer from truncated cones with variable wall temperature and concentration in the presence of chemical reaction effect.

On other hand, heat and mass transfer occurs simultaneously, affecting each other and leading to the Soret and Dufour cross diffusion effects. The molecular transport effects from which species concentrations diffuse due to a temperature gradient (Soret effect, or ‘‘thermal-diffusion’’) and thermal energy diffusion due to a concentration gradient (Dufour effect, or ‘‘diffusion-thermo’’) have been found in real fluids by (Eckert and Drake 1972). Li *et al.* (2006) used an implicit finite-volume method to investigate thermal-diffusion (Soret) and diffusion-themo (Dufour) effects in a strongly endothermic chemically-reacting flow in a porous medium. Postelnicu (2007) has discussed the influence of chemical reaction on heat and mass transfer by natural convection from vertical surfaces embedded in fluid-saturated porous medium considering Soret and Dufour effects. Bég *et al.* (2009) have analyzed the heat and mass transfer by free convection from a stretching surface to a saturated porous medium with Soret and Dufour effects. EL-Kabeir *et al.* (2010) considered the thermal-diffusion and diffusion-thermo effects on heat and mass transfer by MHD mixed convection stagnation-point flow of power law fluid towards a stretching surface in the presence of chemical reaction. Reddy and Rao (2012) have analyzed the Soret and Dufour effects on heat and mass transfer by mixed convection about a circular cylindrical annulus in a porous medium. The effects of diffusion-thermo and thermal-diffusion on heat and mass transfer by MHD free convection along a vertical flat plate with streamwise temperature and the species concentration were investigated by Chamkha *et al.* (2013). Rani and Reddy (2013) have studied the influences of Soret and Dufour effects on double diffusive transient free convective boundary layer flow of a couple-stress fluid flowing over a semi-infinite vertical cylinder. Gangadhar (2013) examined the Soret and Dufour effects on heat and mass transfer over a vertical plate in the presence of chemical reaction and a convective heat exchange at the surface. Chamkha and Rashad (2014) have studied the Soret and Dufour effects on unsteady coupled heat and mass transfer by mixed convection flow over a vertical cone rotating in an ambient fluid in the presence of chemical reaction effect. Rashad and Chamkha (2014) have also investigated the Soret and Dufour Effects on heat and mass transfer by natural convection flow about a truncated cone in porous media.

However, there are numerous practical applications for industrial processes, but there are still relatively few published articles focused on this issue. Therefore, the objective of this article is to discuss simultaneous heat and mass transfer by unsteady three dimensional natural convection flow over a semi-infinite inclined permeable surface embedded in porous medium in the presence of chemical reaction, thermal-diffusion and the diffusion-thermo effects. The order of chemical reaction in this work is taken as first-order reaction. The coupled nonlinear parabolic partial differential equations governing the flow and heat and mass transfer problem have been solved numerically using an implicit iterative finite-difference scheme. Numerical results are presented in the form of velocity, temperature and concentration profiles within the boundary layer for different parameters entering into the analysis. Also the effects of the pertinent parameters on the local skin friction coefficients the local Nusselt and Sherwood numbers are also discussed.

2. MATHEMATICAL FORMULATION

Consider the unsteady, laminar, heat and mass transfer by three-dimensional natural convective boundary-layer flow of viscous incompressible Newtonian fluid over a semi-infinite inclined permeable surface embedded in porous medium in the presence of chemical reaction, thermal-diffusion and the diffusion-thermo effects. The surface is assumed to be permeable at the plate surface in the z-direction and linearly stretched in the x-direction with a velocity bx. The y-direction makes an angle α with the horizontal line while the z-direction is normal to the plate surface. In addition, the concentration of diffusing species thermal-diffusion and diffusion-thermal energy effects are taken into account, and a first-order homogeneous chemical reaction is assumed to take place in the flow. The coordinate system and flow model are shown in Fig. 1. All fluid properties are assumed constant except the density in the buoyancy terms of the x- and y-momentum equations. The thermophysical properties of the fluid and porous media are constant. All dependent variables will be independent of the y-direction, including the Darcy term and chemical term, boundary-layer and Boussinesq approximations of the governing equations can be written as (see Chamkha (2000) and EL-Kabeir *et al.* (2008)):

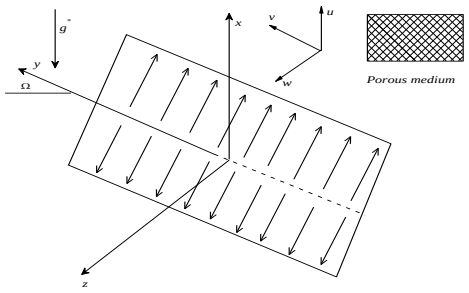

Fig. 1. Flow model and physical co-ordinate system

$$\frac{\partial u}{\partial x}+\frac{\partial w}{\partial z}=0\,, \tag{1}$$

$$\frac{\partial u}{\partial t}+u\frac{\partial u}{\partial x}+w\frac{\partial u}{\partial z}=\nu\frac{\partial^2 u}{\partial z^2}+ g^*\cos\Omega\left[\beta_T(T-T_\infty)+\beta_C(C-C_\infty)\right]-\frac{\nu}{K}u\,, \tag{2}$$

$$\frac{\partial v}{\partial t}+w\frac{\partial v}{\partial z}=\nu\frac{\partial^2 v}{\partial z^2}+ g^*\sin\Omega\left[\beta_T(T-T_\infty)+\beta_C(C-C_\infty)\right]-\frac{\nu}{K}v\,, \tag{3}$$

$$\frac{\partial w}{\partial t}+w\frac{\partial w}{\partial z}=-\frac{1}{\rho}\frac{\partial P}{\partial z}+\nu\frac{\partial^2 w}{\partial z^2}-\frac{\upsilon}{K}w\,, \tag{4}$$

$$\frac{\partial T}{\partial t}+w\frac{\partial T}{\partial z}=\frac{\upsilon}{\Pr}\frac{\partial^2 T}{\partial z^2}+\frac{D_m K_T}{C_s C_p}\frac{\partial^2 C}{\partial z^2}\,, \tag{5}$$

$$\frac{\partial C}{\partial t}+w\frac{\partial C}{\partial z}=\frac{\upsilon}{Sc}\frac{\partial^2 C}{\partial z^2}+\frac{D_m K_T}{T_m}\frac{\partial^2 T}{\partial z^2}-K_1(C-C_\infty) \tag{6}$$

where *x*, *y*, and *z* are the coordinate directions. *u*, *v*, *w*, *P*, *T* and *C* are the fluid velocity components in the *x*, *y*, and *z* directions, pressure, temperature and concentration, respectively. β_T is the coefficient of the thermal expansion; β_C is the coefficient of the concentration expansion. ρ,υ, C_p, and D_m are the fluid density, kinematic viscosity, specific heat at constant pressure, and the mass diffusivity, respectively. g^*, *b*, *t*, C_∞, and Ω are the gravitational acceleration, constant, dimensional time, ambient concentration, and the inclination angle, respectively. *K* and K_1 are the permeability of porous medium and chemical reaction rate, respectively. T_m, K_T and C_s are the mean fluid temperature, thermal diffusion ratio and concentration susceptibility; $\Pr=\upsilon/\alpha$ and $Sc=\upsilon/D_m$ are the effective Prandtl number and Schmidt number, respectively. The last term on the right-hand side of each of the energy Eq. (3) and the diffusion Eq. (4) signifies the Dufour or diffusion-thermo effect and the Soret or thermal-diffusion effect, respectively.

The appropriate boundary conditions for this problem can be written as

$$\begin{aligned}&u(t,x,0)=bx, v(t,x,0)=0, w(t,x,0)=w_0,\\ &T(t,x,0)=T_w, C(t,x,0)=C_w, \frac{\partial w}{\partial z}(t,x,0)=0,\\ &u(t,x,\infty)=0, v(t,x,\infty)=0,\\ &T(t,x,\infty)=T_\infty, C(t,x,\infty)=C_\infty.\end{aligned} \tag{7}$$

where w_0 and T_w are the wall suction or injection velocity and temperature, respectively. In order to minimize the numerical efforts to solve the governing equations, the following transformations are introduced:

$$\begin{aligned}&\tau=bt\,,\ \eta=z/\sqrt{\nu t}\,,\ u=bxf'(\tau,\eta)+\Gamma\cos\alpha\, g(\tau,\eta)\\ &,\ v=\Gamma\sin\alpha\, h(\tau,\eta)\,,\ w=-\sqrt{b^2\nu t}\,f\,,\\ &\Gamma=\frac{g^*\beta_T(T_w-T_\infty)}{b}\,,\\ &\theta(\tau,\eta)=(T-T_\infty)/(T_w-T_\infty)\,,\\ &\phi(\tau,\eta)=(C-C_\infty)/(C_w-C_\infty)\,,\\ &P=\rho b\nu G(\tau,\eta)\,.\end{aligned} \tag{8}$$

Substituting the variables in Eqs. (8) into Eqs. (1) to (7) leads the following non-dimensional equations:

$$f'''+\frac{\eta}{2}f''+\tau\left(ff''-f'^2-\frac{1}{Da}f'\right)-\tau\frac{\partial f'}{\partial\tau}=0\,, \tag{9}$$

$$g''+\frac{\eta}{2}g'+\tau\left(fg'-f'g-\frac{1}{Da}g+\theta+\Lambda\phi\right)-\tau\frac{\partial g}{\partial\tau}=0\,, \tag{10}$$

$$h''+\frac{\eta}{2}h'+\tau\left(fh'-\frac{1}{Da}h+\theta+\Lambda\phi\right)-\tau\frac{\partial h}{\partial\tau}=0\,, \tag{11}$$

$$G'+f''+\frac{\eta}{2}f'-\frac{1}{2}f+\tau\left(ff'-\frac{1}{Da}f\right)-\tau\frac{\partial f}{\partial\tau}=0 \tag{12}$$

$$\frac{1}{\Pr}\theta''+\frac{\eta}{2}\theta'+\tau f\,\theta'+Du\,\phi''-\tau\frac{\partial\theta}{\partial\tau}=0\,, \tag{13}$$

$$\frac{1}{Sc}\phi''+\frac{\eta}{2}\phi'+\tau(f\,\phi'-\gamma\phi)+Sr\,\theta''-\tau\frac{\partial\phi}{\partial\tau}=0\,, \tag{14}$$

where a prime denotes partial differentiation with respect to η and $\Lambda=\frac{\beta_C(C_w-C_\infty)}{\beta_T(T_w-T_\infty)}$, $Da=Kb/\upsilon$ are the buonacy ratio and Darcy number, respectively. $Du=\frac{D_m K_T(C_w-C_\infty)}{C_s C_p\nu(T_w-T_\infty)}$ is the Dufour number, $Sr=\frac{D_m K_T(T_w-T_\infty)}{\nu T_m(C_w-C_\infty)}$ is the Soret number, $\gamma=K_1/b$ and $f_w=-w_0/\sqrt{b\upsilon}$ are the dimensionless chemical reaction parameter, and wall mass transfer coefficient, respectively. It is should be noted that positive values of f_w indicate fluid suction at the plate surface while negative values of f_w indicate fluid blowing or injection at the wall. In addition, it is clear that the advantage of employing the transformations (7) is that they reduce the number of independent variables by one and that similarity equations are obtained at τ=0. In

this way, the initial profiles or conditions for f', g, h, θ and ϕ are obtained by solving these similar equations subject to the boundary conditions.

The dimensionless boundary conditions become:

$$\begin{aligned} &f(\tau,0)=f_w, f'(\tau,0)=1, g(\tau,0)=0,\\ &h(\tau,0)=0, \theta(\tau,0)=\phi(\tau,0)=1,\\ &f'(\tau,\infty)=g(\tau,\infty)=0,\\ &h(\tau,\infty)=\theta(\tau,\infty)=\phi(\tau,\infty)=0. \end{aligned} \quad (15)$$

Important physical parameters for this flow and heat transfer situation are the skin-friction coefficients in the *x* and *y* directions and the local Nusselt number. The shear stresses at the stretching surface are given by

$$\tau_{zx} = \mu\frac{\partial u}{\partial z}(x,0,t)$$

$$= \frac{\mu}{\sqrt{\upsilon t}}\left(bxf''(\tau,0)+\Gamma\cos\Omega g'(\tau,0)\right), \quad (16)$$

$$\tau_{zy} = \mu\frac{\partial v}{\partial z}(t,x,0) = \frac{\mu}{\sqrt{\upsilon t}}\Gamma\sin\Omega h'(\tau,0), \quad (17)$$

Where $\mu=(\rho\upsilon)$ is the dynamic viscosity of the fluid. Upon quantities of τ_{zx} and τ_{zy} by $\mu=\rho(bx)^2/2$, the following respective expressions for the skin-friction coefficients in the x and y directions result:

$$C_{fx} = \frac{2x}{\mathrm{Re}_x\sqrt{\upsilon t}}\left(f''(\tau,0)+\frac{Gr_x}{\mathrm{Re}_x^2}\cos\Omega g'(\tau,0)\right) \quad (18)$$

$$C_{fy} = \frac{2xGr_x}{\mathrm{Re}_x^3\sqrt{\upsilon t}}\sin\Omega h'(\tau,0), \quad (19)$$

Where $Gr_x = g^*\beta_T(T_w-T_\infty)x^3/\upsilon^2$ and $\mathrm{Re}_x = bx^2/\upsilon$ are the local Grashof and Reynolds number, respectively.

The wall heat transfer is given by as follows;

$$q_w = -k\frac{\partial T}{\partial z}(t,x,0) = -\frac{k}{\sqrt{\upsilon t}}(T_w-T_\infty)\theta'(\tau,0), \quad (20)$$

and then, the local Nusselt number for this situation can then be defined as

$$Nu_x = \frac{q_w x}{k(T_w-T_\infty)} = -\frac{x}{\sqrt{\upsilon t}}\theta'(\tau,0), \quad (21)$$

The wall mass transfer is given by;

$$m_w = -D_m\frac{\partial C}{\partial z}(t,x,0) = -\frac{D_m}{\sqrt{\upsilon t}}(C_w-C_\infty)\varphi'(\tau,0) \quad (22)$$

The local Sherwood number can be defined as

$$Sh_x = \frac{m_w x}{D_m(C_w-C_\infty)} = -\frac{x}{\sqrt{\upsilon t}}\varphi'(\tau,0), \quad (23)$$

3. NUMERICAL METHOD

The initial-value problem represented by Eqs. (9) to (14) is nonlinear and possesses no analytical solution. Therefore, a numerical solution is sought for this problem. The standard implicit, iterative, finite-difference method discussed by Blottner (1970) has proven to be adequate and accurate for this type of problems and therefore, it is chosen for the solution of Eqs. (9) to (14) subject to Eqs. (15). The computational domain is divided into 501 by 196 nodes in the τ and η directions, respectively. This gave η_∞=35 and τ_∞=5.0. The independence of the results from the grid density was ensured and successfully checked by various trial and error numerical experimentations. Since the changes in the dependent variables are large in the immediate vicinity of the surface and at the start of the flow. The initial step sizes employed were $\Delta\eta_1$ = 0.001 and $\Delta\tau_1$= 0.01 and the growth factors were K_η = 1.0375 and K_τ= 1.0 such that $\Delta\eta_n = K_\eta\,\Delta\eta_{n-1}$ and $\Delta\tau_m = K_\tau\,\Delta\tau_{m-1}$. The convergence criterion used was based on the relative difference between the current and the previous iterations which was set to 10^{-5} in the present work. For more details on the numerical procedure, the reader is advised to read the paper by Blottner (1970).

4. RESULTS AND DISCUSSION

Figures 2 to 23 represent typical numerical results based on the solution of Eqs. (9) to (14). These results are obtained to illustrate the influences of the Darcy number *Da*, Dufour number *Du*, Soret number *Sr*, blowing/injection parameter f_w and the dimensionless chemical reaction parameter γ on the profiles of the transient fluid velocities flow, temperature and the solute concentration as well as the transient developments of the local skin-friction coefficients in the *x* and *y* directions C_{fx} and C_{fy}, local Nusselt number Nu_x and the local Sherwood number Sh_x. It should be mentioned that in all the results, computations were carried out for various values of parameters, the value of Prandtl number Pr = 0.71 which corresponds physically to air and the value of Schmidt number *Sc*=0.22 (hydrogen at 25 degrees Celsius and 1 atmosphere pressure.) which represents the most common diffusing chemical species. Also, the value of the corresponding buoyancy force parameter (ratio of the buoyancy force due to mass diffusion to the buoyancy force due to the thermal diffusion) N takes the value 1.0 for low concentration. Such data therefore corresponds to hydrogen gas diffusing in air percolating in a porous medium under the action of weak thermal and species buoyancy forces. Moreover, the values of Dufour and Soret numbers are chosen in such a way that their product is constant provided that the mean temperature T_m is kept constant as well. The results of this parametric study are shown in Figs. 2 to 23.

Figures 2 to 7 illustrate the effects of the blowing/injection parameter f_w, on the profiles of the fluid velocity components in *x*-direction f' and

g, velocity component in *y*-direction *h*, pressure *G*, temperature θ and the fluid concentration ϕ with various values of the Dufour number (diffusion-thermal effect) *Du* and Soret number (thermo-diffusion effect) *Sr*, respectively.

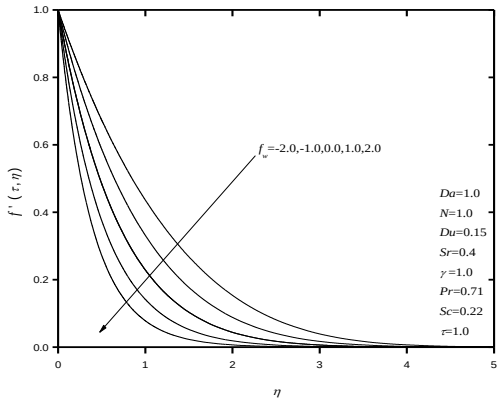

Fig. 2. Effect of blowing/suction parameter f_w on the fluid velocity of *x*-direction (f').

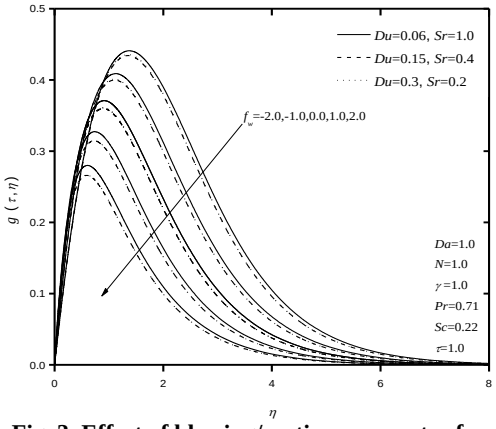

Fig. 3. Effect of blowing/suction parameter f_w , Soret and Dufour numbers on the fluid velocity of x-*direction* (g).

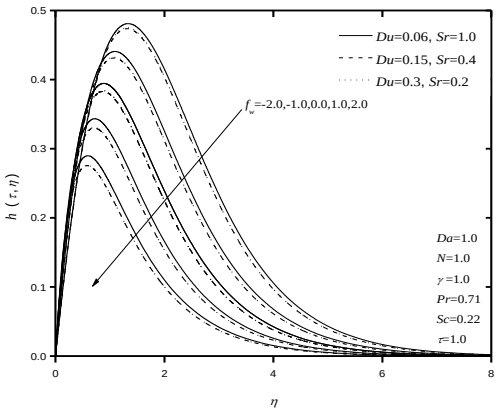

Fig. 4. Effect of blowing/suction parameter f_w Soret and Dufour numbers on the fluid velocity of *y*-direction (*h*).

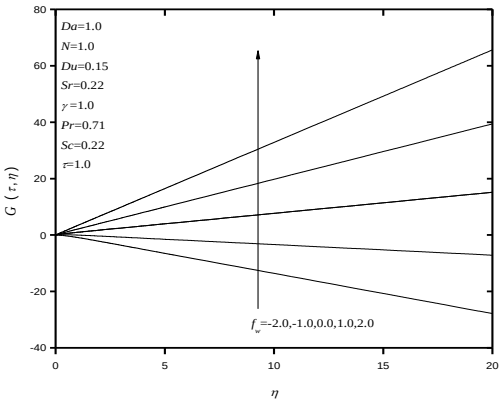

Fig. 5. Effect of blowing/suction parameter f_w on the pressure profiles (*G*).

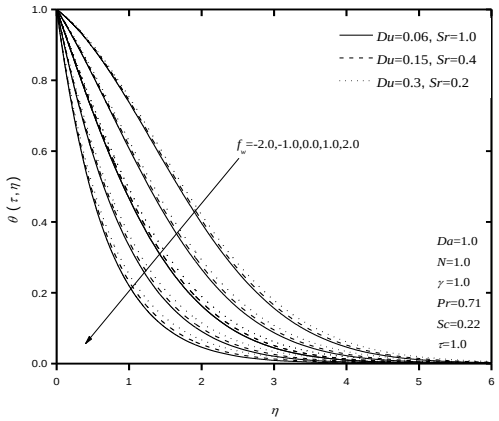

Fig. 6. Effects of blowing/suction parameter f_w, Soret and Dufour numbers on the fluid temperature (θ).

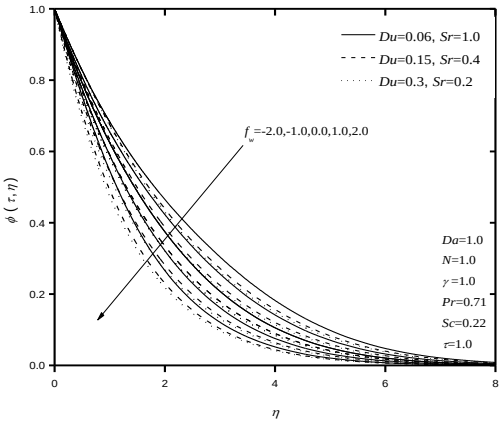

Fig. 7. Effects of blowing/suction parameter f_w, Soret and Dufour numbers on the fluid concentration (ϕ).

It can be seen that, an imposition of wall fluid suction (f_w >0) tends to decelerate the flow at stretched surface, with reduced both the fluid temperature and concentration profiles, whereas an imposition of fluid injection or blowing at the permeable surface (f_w<0) produces the opposite behavior, namely, an increase in the flow velocity and increases in the temperature. Therefore, an increase in the values of blowing/injection

parameter f_w causes increasing the fluid pressure profile G, whereas decreasing in the fluid's velocity components in the x- and y- directions, fluid temperature and concentration profiles, more warm fluid is taken away, and thus the thermal boundary layer thickness decreases. On the other hand, It is indicated that the x and y velocity components and concentration profiles increase with increasing the value of Sr (or decreasing Du), whereas the fluid temperature decreases as Sr increases (or Du decreases). It is noticed that this behavior is a direct consequence of the Soret effect, which produces a mass flux from lower to higher solute concentration driven by the temperature gradient. This because the decreasing Du clearly reduces the influence of species gradients on the temperature field, so that its boundary layer regime is cooled, and mass diffusion is enhanced in the domain as a result of the contribution of temperature gradients. These behaviors are clearly depicted in Figs. 2 to 7. In addition, it is obvious that the governing Eqs. (9) to (14) are uncoupled. Therefore, changes in the values of Du and Sr will cause no changes in both of the distributions of the velocity component in the x-direction f', and the fluid pressure G, and for this reason, no figures for these variables are presented herein.

Figures 8 to 12 show the effects of the blowing/injection parameter f_w on the local skin-friction coefficients in the x- and y- directions C_{fx} and C_{fy}, local Nusselt number Nu_x and the local Sherwood number Sh_x, respectively. As seen from the definitions of C_{fx}, C_{fy}, Nu_x and Sh_x, they are directly proportional to $f''(\tau,0)$, $g'(\tau,0)$, $h'(\tau,0)$, $-\theta'(\tau,0)$ and $-\phi'(\tau,0)$, respectively. From these Figs., it can be seen that as the blowing/injection parameter f_w increases all the skin-friction coefficients, local Nusselt number Nu_x and local Sherwood number Sh_x enhance. The lower flow velocities and temperatures resulting from application of fluid suction at the surface are followed by decreases in the wall slopes of the fluid velocity components in x-direction f' and g, velocity component in y-direction h, temperature θ and the fluid concentration ϕ or higher values of heat transfer rate $-\theta'(\tau,0)$ and mass transfer rate $-\phi'(\tau,0)$ at every time. However, the opposite effect is obtained for wall fluid blowing or injection. It should be noted that the wall heat transfer $-\theta'(\tau,0)$ is more responsive to suction than injection as it increases sharply with time as is clear from Fig. 11.

Furthermore, increasing the value of Sr (or decreasing Du) causes decreases in the mass transfer rate $-\phi'(\tau,0)$ and increases in the heat transfer rate $-\theta'(\tau,0)$, the skin-friction coefficients in the x- and y-directions $g'(\tau,0)$, $h'(\tau,0)$. This is basically due to the fact that the mass diffusion is evidently enhanced in the domain as a result of the contribution of temperature gradients. This result means that the Dufour and Soret effects may play a significant role for intermediate molecular weight gases in coupled heat and mass transfer in binary systems, often encountered in chemical process engineering. Moreover, since the Soret effect appears in the concentration Eq. (14), the changes in the mass transfer rate that are brought about by changing Sr are much more significant than those in the local Nusselt number. Also, no effect on the skin-friction coefficient in the x-direction $f''(\tau,0)$ for the same reason as obvious above. These behaviors are evident from Figs. 8 to 12.

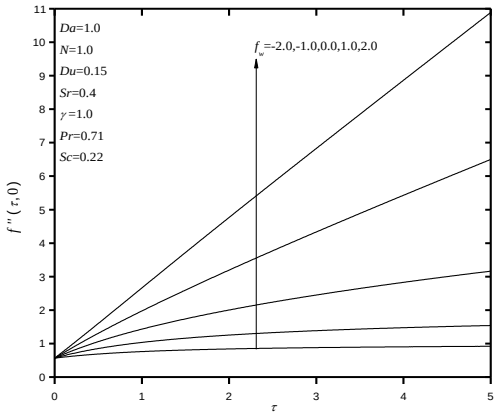

Fig. 8. Effect of blowing/suction parameter f_w on the skin-friction coefficient in the x-direction $f''(\tau,0)$.

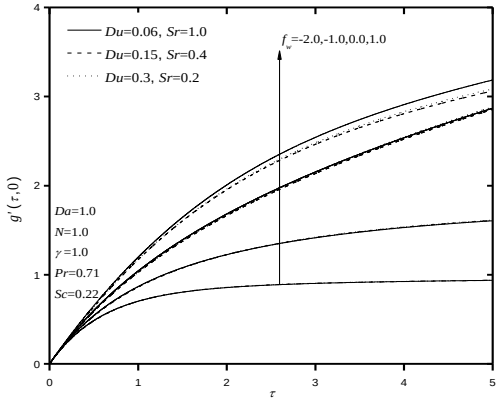

Fig. 9. Effects of blowing/suction parameter f_w, Soret and Dufour numbers on the skin-friction coefficient in the x-direction $g'(\tau,0)$.

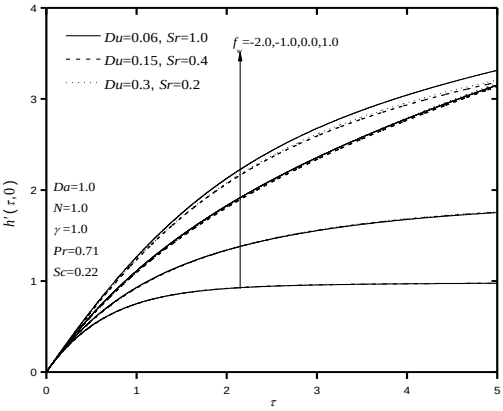

Fig. 10. Effects of blowing/suction parameter f_w, Soret and Dufour numbers on the skin-friction coefficient in the y-direction $h'(\tau,0)$.

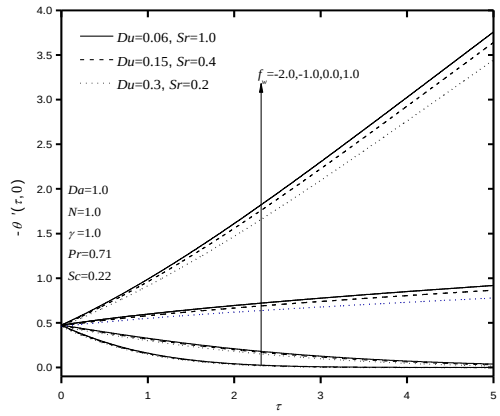

Fig. 11. Effects of blowing/suction parameter f_w, Soret and Dufour numbers on the wall heat transfer $-\theta'(\tau,0)$.

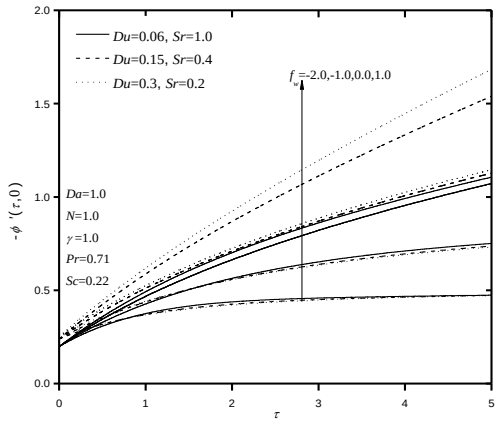

Fig. 12. Effects of blowing/suction parameter f_w, Soret and Dufour numbers on the wall mass transfer $-\varphi'(\tau,0)$.

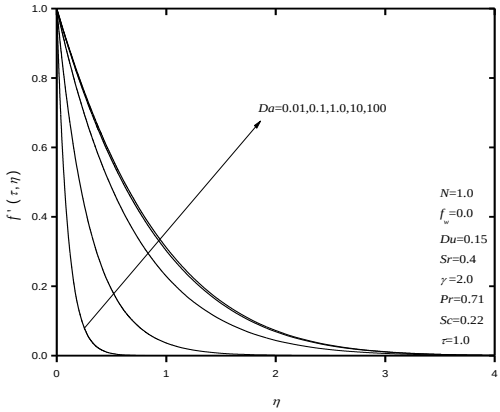

Fig. 13. Effect of Darcy number *Da* on the fluid velocity of *x*-direction (f').

The effects of the chemical reaction γ and Darcy number *Da* on the components of velocities flow, fluid temperature and concentration profiles are shown in Figs. 13 to 18, respectively. It is seen that both the *x* and *y*-components of velocity and concentration profiles decrease with the increase of the chemical reaction parameter γ, while insignificant increases in the temperature profiles occurs. This shows that the diffusion rates can be tremendously altered by chemical reactions. It is evident that increasing the chemical reaction parameter significantly alters the thermal and concentration boundary layers thickness without any significant effect on the momentum boundary layers.

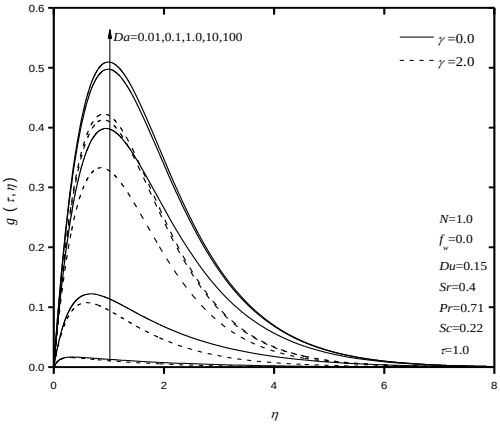

Fig. 14. Effects of Darcy number *Da* and chemical reaction parameter γ on the fluid velocity of *x*-direction (*g*).

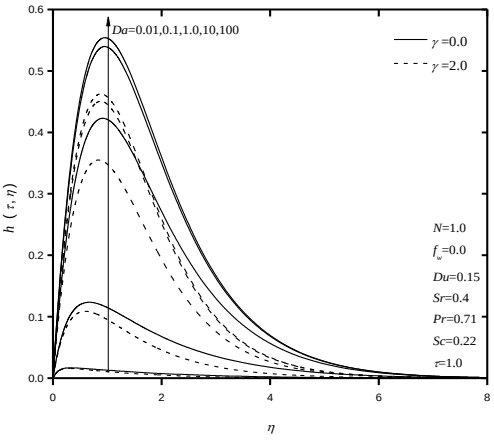

Fig. 15. Effects of Darcy number *Da* and chemical reaction parameter γ on the fluid velocity of *y*-direction (*h*).

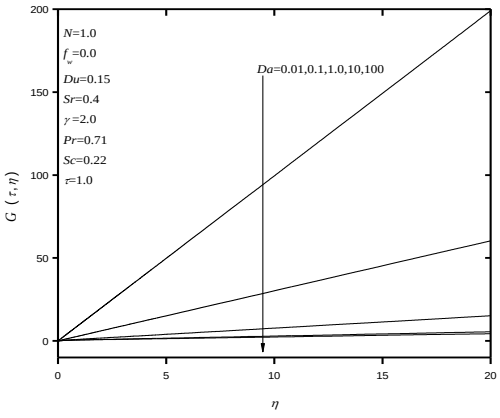

Fig. 16. Effect of Darcy number Da on the pressure profiles (G).

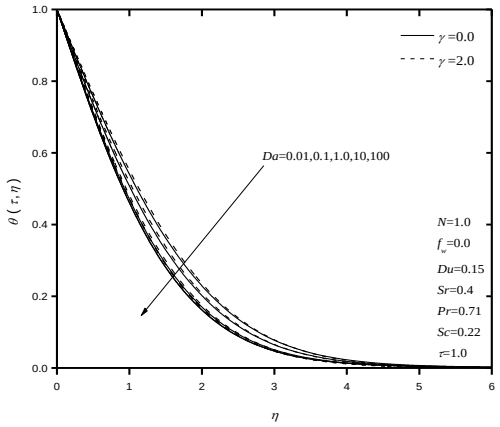

Fig. 17. Effects of Darcy number *Da* and chemical reaction parameter γ on the fluid temperature (θ).

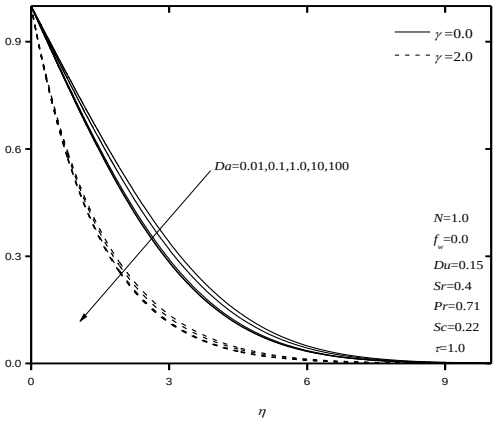

Fig. 18. Effects of Darcy number *Da* and chemical reaction parameter γ on the fluid concentration (ϕ).

On other side, it is found that an increase in Darcy number *Da* from 0.01 through 0.1, 1.0, 10 to 100 (very high permeability) clearly leads to enhance in the *x*-velocity components (f' and g) and *y*-velocity component *h*, i.e., accelerates the flow. The changes in velocity are maximized some distance from the wall, towards the free stream. As such the fluid acceleration towards the edge of the boundary layer is less impeded by wall effects here. Also, with higher *Da* values there will be a corresponding reduction in the Darcian drag force, due to the inverse relationship in Eqs. (9) and (10) and this will serve to effectively accelerate the flow in the medium along to the stretching surface Therefore, this acceleration in the flow leads to a marked reduction in the fluid temperature, concentration and the pressure profiles *G*. In addition, it can be seen that an increasing in the values of *Da* are followed by corresponding reduces in all hydrodynamic, thermal and solutal (concentration) boundary layers.

The variations of the local skin-friction coefficients and the local Nusselt and Sherwood numbers against the chemical reaction parameter γ and and Darcy number *Da* are shown in Figs 19 to 23, respectively. It can be seen that as γ increases, the local Sherwood number increases while the opposite effect is found for both of the local skin-friction coefficient and the local Nusselt number. This is because as γ increases, the concentration difference between the surface and the fluid decreases and so the rate of mass transfer at the surface must increase while all the local skin-friction coefficients in the *x*- and *y*-directions and the rate of heat transfer decreases as a result of the decrease in the flow velocity and fluid temperature, respectively. However, the variation of chemical reaction parameter in this problem can play an important role on the mass transfer and it is clearly observed in many processes such as drying, distribution of temperature and moisture over agricultural fields and groves of fruit trees, damage of crops due to freezing, evaporation at the surface of a water body, energy transfer in a wet cooling tower and flow in a desert cooler, heat and mass transfer occur simultaneously.

On other side, it is observed form Figs. 19 to 23 that there are two opposite behaviors for the coefficient of surface shear stress and both the rates of heat and mass transfer. This is because the presence of a porous medium in the flow provides resistance to flow. Thus, the resulting resistive force tends to slow down the motion of the fluid along the cone surface and causes increases in its temperature and concentration.

These behaviors yields a reduction in the skin-friction coefficient in the *x*-direction $f''(\tau,0)$ and the enhancement in the skin-friction coefficients in the *x*- and *y*-directions $g'(\tau,0)$, $h'(\tau,0)$ and both of the rates of heat and mass transfer as a result of increasing the Darcy number *Da*. This phenomenon may interest in many engineering and geophysical applications such as geothermal reservoirs, drying of porous solids, enhanced oil recovery, packed bed catalytic reactors, cooling of nuclear reactors, and underground energy transport.

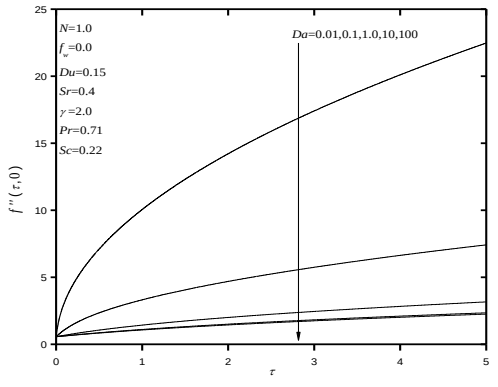

Fig. 19. Effect of Darcy number *Da* on the skin-friction coefficient in the *x*-direction $f''(\tau,0)$.

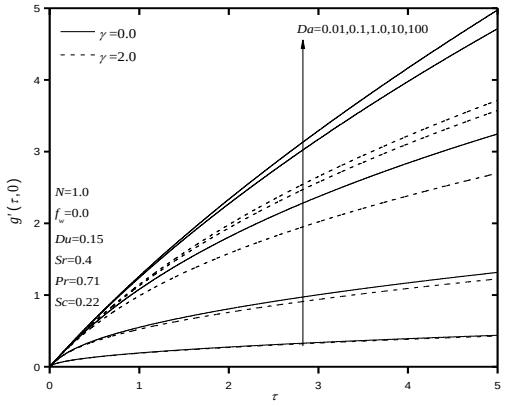

Fig. 20. Effects of Darcy number *Da* and chemical reaction parameter γ on the skin-friction coefficient in the *x*-direction $g'(\tau,0)$.

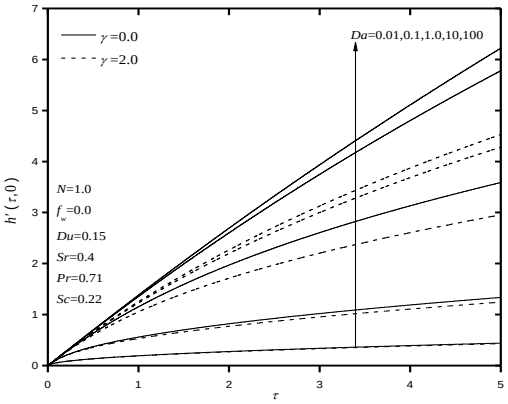

Fig. 21. Effects of Darcy number *Da* and chemical reaction parameter γ on the skin-friction coefficient in the *y*-direction $h'(\tau,0)$.

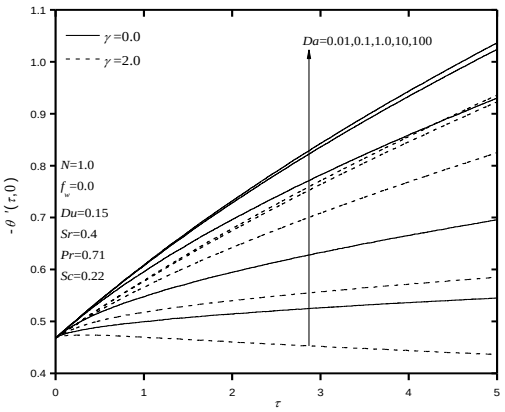

Fig. 22. Effects of Darcy number *Da* and chemical reaction parameter γ on the wall heat transfer $-\theta'(\tau,0)$.

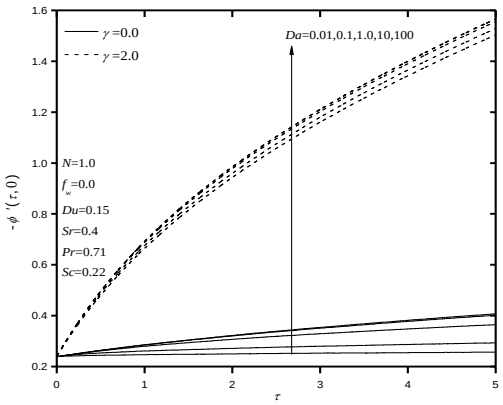

Fig. 23. Effects of Darcy number *Da* and chemical reaction parameter γ on the wall mass transfer $-\varphi'(\tau,0)$.

5. CONCLUSION

This work considered coupled heat and mass transfer by unsteady three dimensional natural convection boundary-layer flow of viscous incompressible Newtonian fluid over a semi-infinite inclined permeable surface embedded in porous medium in the presence of chemical reaction, thermal-diffusion and the diffusion-thermo effects. The surface is assumed to be permeable at the plate surface in the *z*-direction and linearly stretched in the *x*-direction. The governing equations were formulated and transformed into a set of similar equations. These equations were solved numerically by an implicit, iterative, tri-diagonal, finite-difference method. Numerical results for the velocity, temperature, and concentration profiles as well as the local skin-friction coefficients, local Nusselt number and local Sherwood number were reported graphically. It was found that imposition of fluid wall suction increased the transient wall heat and mass transfer distributions as well as the time history of the skin-friction coefficients in both the *x*- and *y*-directions. In addition, the increasing the values of Darcy number was found to be enhancing the local Nusselt and Sherwood numbers and the skin-friction coefficient in the *y*-direction while reducing the skin-friction coefficient in the *x* direction at any time. However, increases in the values of either of the chemical reaction parameter or the Dufour number (diffusion-thermal effect) produced decreases in the skin-friction coefficients in both the *x* and y directions and local Nusselt number and increases in the local Sherwood number. However, the opposite behavior was predicted as the Soret number (thermo-diffusion effect) was increased for which the local Nusselt number was increased while the local Sherwood number was decreased.

ACKNOWLEDGMENT

The authors gratefully acknowledge Research Centre, Salman bin Abdulaziz University, Kingdom of Saudi Arabia, for supporting and encouragement during this research project, no. 4T33.

REFERENCES

Bég, O.A., A. Y. Bakierand, and V. R. Prasad. (2009). Numerical study of free convection magnetohydrodynamic heat and mass transfer from a stretching surface to a saturated porous medium with Soret and Dufour effects. *Computational Materials Science*, 46, 57-65.

Blottner, F. G. (1970). Finite-difference methods of solution of the boundary-layer equations. *AIAA J.*, 8, 93-205.

Chamkha, A. J. (2000). Transient hydromagnetic three-dimensional natural convection from an inclined stretching permeable surface. *Chem. Eng. Journal*, 76, 159-168.

Chamkha, A. J. and A. M. Rashad (2014). Unsteady heat and mass transfer by MHD mixed convection flow from a rotating vertical cone with chemical reaction and Soret and Dufour effects. *Canadian Journal of Chemical Engineering* 92(4), 758-767.

Chamkha, A. J., S. M. M. EL-Kabeir, and A. M. Rashad (2011). Heat and mass transfer by non-Darcy free convection from a vertical cylinder embedded in porous media with a temperature-dependent viscosity. *Int. J. Numerical Methods for Heat and Fluid Flow* 21(7), 847-863.

Chamkha, A. J., S. M. M. EL-Kabeir, and A. M. Rashad (2013). Coupled heat and mass transfer by MHD free convection flow along a vertical plate with streamwise temperature and species concentration variations. *Heat Transfer-Asian Research* 42(2), 100-110.

Chamkha, A. J., A. M. Rashad, and H. Al-Mudhaf (2012). Heat and mass transfer from truncated cones with variable wall temperature and concentration in the presence of chemical reaction effects. *Int. J. Numerical Methods for Heat and Fluid Flow* 22 (3), 357-376.

Das, U. N., R. Deka, and V. M. Soundalgekar(1994). Effects of mass transfer on flow past an impulsive started infinite vertical plate with constant heat flux and chemical reaction. *Forschung Im Ingenieurwesen-Engineering Research Bd*, 60, 284-287.

Eckert, E. R. G. and R. M. Drake (1972). *Analysis of Heat and Mass Transfer*, McGraw-Hill, New York.

EL-Kabeir, S. M. M., A. J. Chamkha, and A. M. Rashad, (2010). Heat and mass transfer by MHD stagnation-point flow of a power-law fluid towards a stretching surface with radiation, chemical reaction and Soret and Dufour effects. *Int. J. Chemical Reactor Engineering*, 8, 1-18.

EL-Kabeir, S. M. M., M. A. EL-Hakiem, and A. M. Rashad (2008). Lie group analysis of unsteady MHD three dimensional by natural convection from an inclined stretching surface saturated porous medium. *J. Computational Applied Mathematics*, 213, 582-603.

Fairbanks, D. F. and C. R. Wike (1950). Diffusion and chemical reaction in an isothermal laminar flow along a soluble flat plate. *Ind. Eng. Chem. Res.* 42, 471-475.

Gangadhar, K. (2013). Soret and Dufour effects on hydro magnetic heat and mass transfer over a vertical plate with a convective surface boundary condition and chemical reaction. *Journal of Applied Fluid Mechanics* 6(1), 95-105.

Ingham, D.B. and I. Pop (Eds.), (1998), vol. II, (2002). *Transport Phenomena in Porous Media*, Pergamon, Oxford.

Li, M-C., Y-W. Tian, and Y-C-. Zhai (2006). Soret and Dufour effects in strongly endothermic chemical reaction system of porous media. *Trans. Nonferrous Metals Society China* 16(5), 1200-1204.

Modather, M. and A. M. Rashad. and A. J. Chamkha (2009). An analytical study on MHD heat and mass transfer oscillatory flow of micropolar fluid over a vertical permeable plate in a porous medium. *Turkish J. Eng. Env. Sci.*, 33, 245-257.

Muthucumaraswamy, R., N. Dhanasekar and Prasad, G.E. (2013). Rotation effects on unsteady flow past an accelerated isothermal vertical plate with variable mass transfer in the presence of chemical reaction of first order. *Journal of Applied Fluid Mechanics* 6(4), 485-490.

Muthucumarswamy, R. and P. Ganesan, (2001). First order chemical reaction on flow past an impulsively started vertical plate with uniform heat and mass flux. *Acta Mech*, 147, 45-57.

Nield, D.A. and A. Bejan, (2006). *Convection in Porous Media*, third Ed., Springer, New York.

Pop, I. and D. B. Ingham (2001). *Convective Heat Transfer: Mathematical and Computational Modelling of Viscous Fluids and Porous Media*, Pergamon, Oxford.

Postelnicu, A. (2007). Influence of chemical reaction on heat and mass transfer by natural convection from vertical surfaces in porous media considering Soret and Dufour effects. *Heat Mass Transfer* 43, 595-602.

Rani, H. P. and G. J. Reddy, (2013). Soret and Dufour effects on transient double diffusive free convection of couple-stress fluid past a vertical cylinder. *Journal of Applied Fluid Mechanics* 6(4), 545-554.

Rashad, A. M. and A. J. Chamkha (2014). Heat and mass transfer by natural convection flow about a truncated cone in porous media with Soret and Dufour effects. *Int. J. Numerical Methods for Heat and Fluid Flow* 24(3), 595-612.

Rashad, A. M. and S. M. M. EL-Kabeir (2010). Heat and mass transfer in transient flow by mixed convection boundary layer over a stretching sheet embedded in a porous medium with chemically reactive species. *Journal of Porous Media*, 13, 75-85.

Rashad, A. M., A. J. Chamkha, and S. M. M. EL-Kabeir (2011). Effect of chemical reaction on heat and mass transfer by mixed convection flow about a solid sphere in a saturated porous media. *Int. J. Numerical Methods for Heat and Fluid Flow* 21(4), 418-433.

Rashad, A. M., M. Modather, and A. J. Chamkha (2011). MHD free convective heat and mass transfer of a chemically-reacting fluid from radiate stretching surface embedded in a saturated porous medium. *International Journal of Chemical Reactor Engineering* 9, 1-15.

Reddy, P. S. and V. P. Rao (2012). Thermo-Diffusion and Diffusion-Thermo effects on convective heat and mass transfer through a porous medium in a circular cylindrical annulus with quadratic density temperature variation-finite element study. *Journal of Applied Fluid Mechanics* 5(4), 139-144.

Vafai, K. (Ed.), (2000). *Handbook of Porous Media*, Marcel Dekker, Marcel.